Journal of Molecular Liquids 434 (2025) 128000

Contents lists available at ScienceDirect

Journal of Molecular Liquids

journal homepage: www.elsevier.com/locate/molliq

Comprehensive theoretical analysis of the solubility of two benzodiazepine drugs in supercritical solvent; thermodynamic and advanced machine learning approaches

Enwa Felix Oghenemaro [a,*], Tawfeeq Alghazali [b], Subasini Uthirapathy [c,*], Hardik Doshi [d], Irfan Ahmad [e,f], K.N. Raja Praveen [g], Anirudh Gupta [h], Deeksha Verma [i], Abhinav Kumar [j,k], Ahmed Hjazi [l]

[a] Delta State University Department of Pharmaceutical Microbiology, Faculty of Pharmacy. PMB 1 Abraka, Delta State, Nigeria
[b] The Islamic University in Najaf, Iraq
[c] Pharmacy Department, Tishk International University, Erbil, Kurdistan Region, Iraq
[d] Marwadi University Research Center, Department of Computer Engineering, Faculty of Engineering & Technology, Marwadi University, Rajkot, Gujarat, India
[e] Central Labs, King Khalid University, AlQura'a, Abha, P.O. Box 960,Saudi Arabia
[f] Department of Clinical Laboratory Sciences, College of Applied Medical Sciences, King Khalid University, Abha, Saudi Arabia
[g] Department of Computer Science and Engineering, School of Engineering and Technology, JAIN (Deemed to be University), Bangalore, Karnataka, India
[h] NIMS School of Allied Sciences and Technology, NIMS University Rajasthan, Jaipur 303121, India
[i] Department of Computer Science and Engineering, Chandigarh Engineering College, Chandigarh Group of Colleges-Jhanjeri, Mohali 140307, Punjab, India
[j] Department of Nuclear and Renewable Energy, Ural Federal University Named after the First President of Russia Boris Yeltsin, Ekaterinburg 620002, Russia
[k] Centre for Research Impact & Outcome, Chitkara University Institute of Engineering and Technology, Chitkara University, Rajpura, 140401, Punjab, India
[l] Department of Medical Laboratory, College of Applied Medical Sciences, Princse Sattam bin Abdulaziz University, Al-Kharj 11942, Saudi Arabia

ARTICLE INFO

Keywords:
Solubility
Supercritical CO_2
Benzodiazepine
Thermodynamic models
Machine learning

ABSTRACT

The pharmaceutical industry is showing growing interest in exploring supercritical CO_2 techniques to develop advanced drug delivery systems. In this regard, assessing the solubility of drugs in supercritical CO_2 under different conditions is a vital parameter. In this study, the solubility of two benzodiazepine family drugs, diazepam and alprazolam, in supercritical CO_2 was theoretically assessed using two distinct thermodynamic approaches; the SRK model, which treats supercritical CO_2 as a gas, and the regular solution model, which considers supercritical CO_2 as a liquid and incorporates various expressions for the solubility parameter. Furthermore, machine learning models, including MLP with various training algorithm, GPR and KNN, were employed to predict the solubility of these drugs. The accuracy of the models for each medicine is validated by comparing their results with previously published experimental solubility data. It was demonstrated that both thermodynamic models successfully model the solubility of these drugs in supercritical CO_2. The SRK model yielded mean *AARD* values of 10.36 for diazepam and 3.15 for alprazolam, while the regular solution model, using a specific expression for the solubility parameter, provided the best fit to the experimental results, with mean *AARD* values of 4.69 for diazepam and 6.97 for alprazolam. Also, it was demonstrated that all intelligent models achieved the highest performance in predicting the solubility of diazepam and alprazolam in supercritical CO_2.

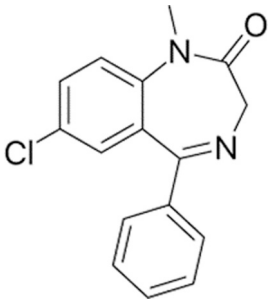
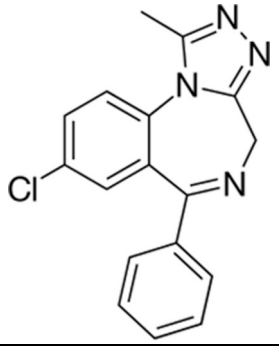
1. Introduction

Numerous studies have confirmed the significant role of pharmaceutical solubility in the body's aqueous environment on the drug therapeutic effectiveness, influencing its absorption, distribution, and overall efficacy [1]. Enhancing a drug solubility can improve its effectiveness and safety by making it easier for the body to absorb. This often allows for lower doses to achieve the same therapeutic effect, thereby reducing the risk of side effects and toxicity. Solubility enhancement is crucial in drug formulation and development. Reducing pharmaceutical particle size to the micro or nano scale is particularly noteworthy among the proposed methods, with support from the Noyes

* Corresponding authors.
E-mail addresses: felixeenwa@gmail.com, felixenwa@delsu.edu.ng (E.F. Oghenemaro).

https://doi.org/10.1016/j.molliq.2025.128000
Received 11 February 2025; Received in revised form 28 May 2025; Accepted 18 June 2025
Available online 26 June 2025
0167-7322/© 2025 Published by Elsevier B.V.

Table 1
Specifications of the pharmaceutical ingredients.

Specifications	Diazepam	Alprazolam
Formula	$C_{16}H_{13}ClN_2O$	$C_{17}H_{13}ClN_4$
Molecular mass ($g.mol^{-1}$)	284.74	308.8
IUPAC name and chemical structure	7-chloro-1,3-dihydro-1-methyl−5-phenyl-2H-1,4-benzodiazepin-2-one 	8-chloro-1-methyl-6-phenyl-4H-triazolo[4,3-a] [1,4] benzodiazepine 

[2] and Ostwald [3] theories. Traditional methods for particle size reduction, such as freeze-drying, milling, and anti-solvent precipitation, face several drawbacks, including high costs, large quantities of organic solvents, high energy consumption, alterations to the original compound properties, inconsistent particle size distribution, and potential mechanical and thermal degradation. These limitations constrain their application in the pharmaceutical industry, highlighting the need for cleaner and more efficient alternatives.

Supercritical methods provide key advantages such as precise solubility control through temperature and pressure adjustments, mild operating conditions essential for temperature-sensitive compounds, and the production of high-purity medicinal compounds with consistent morphology [4–6]. These benefits are driving the growing use of these methods in diverse areas of the medicinal industry. Supercritical CO_2 is widely regarded as the most popular supercritical fluid due to its advantageous properties, such as safety, affordability, non-toxicity, accessibility, environmental friendliness, and relatively mild critical conditions [7–9].

In most supercritical processes, supercritical CO_2 can fulfill two key roles; acting as a solvent for soluble solutes and functioning as an anti-solvent for poorly soluble solutes [10–12]. Consequently, the solubility of the desired pharmaceutical ingredient in supercritical CO_2 is a crucial parameter that must be determined to effectively design a supercritical method [13,14]. However, determining this factor in the laboratory, especially at different temperatures and pressures, is a challenging, time-consuming, and expensive task, which can constrain the practical application of supercritical methods.

To address this challenge, a variety of theoretical approaches have been developed to assess and predict the supercritical solubility of different materials under various operating conditions. These include, **(1)** Density-based semi-empirical models establish a relationship between solubility and temperature, pressure, and the density of the supercritical solvent, with the density being influenced by the temperature and pressure conditions. These models, available in various forms with different numbers of fitting parameters, are among the most widely used and versatile methods successfully used to correlate the supercritical solubility of different substances [14–17]. **(2)** Depending on the equilibrium established between the solute and supercritical CO_2, a range of thermodynamic approaches can be applied to investigate and analyze this equilibrium process, providing insights into solubility and system behavior. For this purpose, two different perspectives have been proposed [18–20]. ***(2a)*** Some researchers treat supercritical CO_2 as a gas and develop fugacity coefficient-based models, where the solute fugacity coefficient is determined using various equations of state (EoSs), which are categorized into cubic and non-cubic types. Cubic EoSs, such as the Soave-Redlich-Kwong (SRK) and Peng-Robinson (PR) models, are represented as cubic functions of molar volume, while non-cubic EoSs are based on the statistical associating fluid theory (SAFT), including models like perturbed chain SAFT (PC-SAFT) and perturbed chain polar SAFT (PCP-SAFT). ***(2b)*** Alternatively, some researchers consider supercritical CO_2 as a liquid and develop activity coefficient-based models, determining the solute activity coefficient using different thermodynamic approaches, such as UNIQUAC and Wilson. **(3)** Intelligent predictive models and machine learning techniques, which are generally more advanced and efficient than earlier models, have been used to predict the solubility of various pharmaceuticals in supercritical CO_2, considering pressure and temperature inputs. There is no established guideline for pinpointing the most accurate model. To identify the best model, it is essential to perform a detailed comparison between the model results and experimental data [21–23].

The main objective of this study is to conduct a comprehensive theoretical assessment of drug solubility in supercritical CO_2 using various thermodynamic and machine learning methods. Two medications, diazepam and alprazolam, from the benzodiazepine family, were selected for this study. They are commonly administered orally and are used to manage panic attacks, generalized anxiety, and depression.

Both the mentioned drugs fall under BCS (Biopharmaceutical Classification System) Class II, where they experience problems with poor solubility and low bioavailability. The physical properties and chemical structure of these drugs are presented in Table 1. The solubility of diazepam in supercritical CO_2 has already been measured under 45 conditions (308 K -348 K, 122 bar −355 bar) [24], while that of alprazolam has been measured under 28 conditions (308 K -338 K, 120 bar −300 bar) [25]. However, a thorough theoretical analysis has not yet been conducted, and existing theoretical studies are typically limited to a few basic semi-empirical models.

This study aims to perform a comprehensive theoretical analysis of the solubility of these drugs in supercritical CO_2. This study utilizes two thermodynamic models, including the SRK equation of state (EoS) for gas-solid equilibrium and the regular solution model for liquid-solid equilibrium. Additionally, it incorporates predictive machine learning techniques, including feed-forward multilayer perceptron (MLP), gaussian process regression (GPR), and k-nearest neighbors (KNN) with political optimizer (PO). The accuracy of the models was assessed by comparing their outputs to previously published experimental data.

2. Thermodynamic methods

2.1. Solid - gas equilibrium thermodynamic model (SRK-EoS)

Determining solute solubility in supercritical CO_2 using different EoSs is based on the equilibrium condition that the fugacity of the solute in the solvent phase must equal its fugacity in the solid phase. Thus, the equilibrium solubility (y_s) was derived using Eq. 1, based on assumptions such as incompressibility, pressure-independent molar volume, purity, low vapor pressure of the solute, and the insolubility of supercritical CO_2 in the solute.

$$y_s = \frac{P_s^{sub}\phi_s^{sat}}{P\phi_s}\exp\left(\frac{v_s\left(P - P_s^{sub}\right)}{RT}\right) \tag{1}$$

Using this relationship, the solubility can be computed at the desired pressure (P) and temperature (T), where v_s is the solute molar volume, ϕ_s^{sat} is the solute saturation fugacity coefficient (assumed to be unity due to the low sublimation pressure of the solute), and ϕ_s is the solute fugacity coefficient in the supercritical CO_2 phase, which is calculated using the following relationship based on the SRK-EoS.

$$RT\ln\phi_i = -RT\ln\frac{PV}{RT} + \int_V^{\infty}\left[\left(\frac{\partial P}{\partial n_i}\right)_{T,V,n_j\neq n_i} - \frac{RT}{V}\right]dV \tag{2}$$

The complete form of the SRK-EoS formula is [26]:

$$P = \frac{RT}{\nu - b} - \frac{a(T)}{\nu(\nu+b)}\begin{cases} a(T) = \dfrac{0.42747R^2T_c^2}{P_c}\left[1 + \left(0.480 + 1.574\omega - 0.176\omega^2\right)\left(1 - T_r^{0.5}\right)\right]^2 \\ b = \dfrac{0.08664RT_c}{P_c} \end{cases} \tag{3}$$

2.2. Solid–liquid equilibrium thermodynamic model (Regular solution model)

The equilibrium solubility of a solute (y_s), where the supercritical CO_2 behaves as a liquid and solubility is extremely low, can be determined using the activity coefficient of the solute at infinite dilution $\left(\gamma_s^{\infty}\right)$, as expressed by the following eq. [28]:

$$y_s = \frac{f_s^{Solid}}{\gamma_s^{\infty} f_s^{Supercritical\ CO_2}} \tag{4}$$

The ratio of solute fugacity in the solid phase to that in the supercritical CO_2 phase $\left(\frac{f_s^{Solid}}{f_s^{Supercritical\ CO_2}}\right)$ is described as a function of the solute enthalpy of melting (ΔH_m), melting point (T_m), and the heat capacity difference between the supercritical and solid phases (ΔC_p). Assuming a constant ΔC_p, the relationship becomes:

$$\ln\left(\frac{f_s^{Solid}}{f_s^{Supercritical\ CO_2}}\right) = \frac{-\Delta H_m}{R}\left(\frac{1}{T} - \frac{1}{T_m}\right) + \frac{\Delta C_p}{R}\ln\left(\frac{T}{T_m}\right) - \frac{\Delta C_p}{RT}\left(\frac{T - T_m}{T}\right) \tag{5}$$

By neglecting ΔC_p, y_s can be obtained through the following simplified relationship:

$$y_s = \frac{1}{\gamma_s^{\infty}}exp\left(\frac{\Delta H_m}{R}\left(\frac{1}{T_m} - \frac{1}{T}\right)\right) \tag{6}$$

In this case, the regular solution model, in conjunction with the Flory–Huggins theory, is utilized to determine γ_s^{∞}, which can be defined as a function of the molar volume (ν) and the solubility parameter (δ) of both the supercritical CO_2 and the solute, as follows [27]:

$$\ln\gamma_s^{\infty} = \frac{\nu_s}{RT}\left(\delta_{supercritical\ CO_2} - \delta_s\right)^2 + 1 - \frac{\nu_s}{\nu_{supercritical\ CO_2}} + \ln\left(\frac{\nu_s}{\nu_{supercritical\ CO_2}}\right) \tag{7}$$

Combining Eq. 6 and Eq. 7:

$$\ln y_s = \frac{\Delta H_m}{R}\left(\frac{1}{T_m} - \frac{1}{T}\right) - \frac{\nu_s}{RT}\left(\delta_{supercritical\ CO_2} - \delta_s\right)^2 - 1 + \left(\frac{\nu_s}{\nu_{supercritical\ CO_2}}\right) - \ln\left(\frac{\nu_s}{\nu_{supercritical\ CO_2}}\right) \tag{8}$$

The parameter $\delta_{supercritical\ CO_2}$ is obtained through the following relationship using reference parameters, including $\delta_{dref} = 15.6\ MPa^{0.5}$, $\nu_{ref} = 39.13\ cm^3.mol^{-1}$, $\delta_{pref} = 5.2\ MPa^{0.5}$, $\delta_{href} = 5.8\ MPa^{0.5}$, and $T_{ref} = 298.15\ K$ [28].

$$\delta^2_{supercritical\ CO_2} = \left[\frac{\delta_{dref}}{\left(\frac{\nu_{ref}}{\nu_{supercritical\ CO_2}}\right)^{-1.25}}\right]^2 + \left[\frac{\delta_{pref}}{\left(\frac{\nu_{ref}}{\nu_{supercritical\ CO_2}}\right)^{-0.5}}\right]^2 + \left[\frac{\delta_{href}}{\exp\left(-1.32\times10^{-3}\left(T_{ref} - T\right) - \ln\left(\frac{\nu_{ref}}{\nu_{supercritical\ CO_2}}\right)^{0.5}\right)}\right]^2 \tag{9}$$

Various formulations based on the reduced density of CO_2 ($\rho_{r,supercritical\ CO_2}$) have been proposed to determine δ_s, as follows [29]:

$$\delta_s = A + B\rho_{r,supercritical\ CO_2} \tag{10}$$

$$\delta_s = A + B\rho^C_{r,supercritical\ CO_2} \tag{11}$$

Table 2
Properties of the desired medicinal substances.

Property		Diazepam	Alprazolam
T_m (K)		403.6 [45]	501.8 [46]
T_b (K)		770.4*	782*
T_c (K)		939.4	1015.5
P_c (bar)		23.91	23.88
H^f (kJ.mol^{-1})		28.0	21.8
ω		0.96	0.98
$\nu^s \times 10^6$ (m^3.mol^{-1})		309.52	321.63
P^{sub} (Pa)	T = 308 K	4.3×10^{-6}	2.6×10^{-7}
	T = 318 K	2.1×10^{-5}	1.35×10^{-6}
	T = 328 K	8.9×10^{-5}	6.4×10^{-6}
	T = 338 K	3.5×10^{-4}	2.7×10^{-5}
	T = 348 K	1.3×10^{-3}	1.1×10^{-4}

* http://www.chemspider.com

$$\delta_s = A + B\rho_{r,\text{supercritical } CO_2} + C\rho^2_{r,\text{supercritical } CO_2} \quad (12)$$

$$\delta_s = A + B\rho_{r,\text{supercritical } CO_2} + CT \quad (13)$$

here, A, B, and C are the fitting parameters.

2.3. Estimating the physicochemical properties of diazepam and alprazolam

As outlined in the relationships presented in Sections 2.1 and 2.2, certain properties of the solute must be known to determine its solubility in supercritical CO_2. These properties include the acentric factor (ω), critical temperature (T_c), critical pressure (P_c), sublimation pressure (P^{sub}), molar volume (v^s), and heat of fusion (H^f), which must be determined using different group contribution methods.

The Marrero - Gani method [30] was chosen to determine T_c, P_c, and H^f for diazepam and alprazolam, as it has been successfully applied to estimate these properties for various drugs, such as azathioprine [31], imatinib mesylate [32], minoxidil [33], febuxostat and chlorpromazine [34], repaglinide [35], gemifloxacin [36], metformin [23], levetiracetam [37], montelukast [38], zolpidem [39], among others. The Immirzi–Perini procedure [40], recognized as one of the most reliable methods for estimation of v^s [13,17,18,41], was chosen to determine this parameter for the selected drugs. The Edmister's method [42] was chosen to determine the ω factor for the desired drugs, as it has already been used effectively to estimate this property for substances such as sodium valproate [43], minoxidil [33], yellow 2G [11], and gemifloxacin [36]. Additionally, for the estimation of P^{sub}, the Mackay et al. [44] approach was chosen due to its reliability and ease of use, as outlined below:

$$\ln P^{sub} = -(4.4 + \ln T_b)\left[1.803\left(\frac{T_b}{T} - 1\right) - 0.803\ln\left(\frac{T_b}{T}\right)\right] - 6.8\left(\frac{T_m}{T} - 1\right) \quad (14)$$

In this relationship, T_b and T_m are the boiling and melting points of the desired substance. The properties estimated for diazepam and alprazolam are listed in Table 2.

3. Machine learning methods

3.1. MLP model

The artificial neural network (ANN) is a well-known machine learning method that effectively models nonlinear relationships by emulating the structure and function of biological neural networks. It comprises multiple neurons acting as computational units, organized into three layers: an input layer, with neurons corresponding to the independent variables; an output layer, where the number of neurons matches the dependent variables; and at least one hidden layer in between, with an adjustable number of neurons that must be optimized. The feed-forward multilayer perceptron (MLP) is one of the most established and widely recognized ANN architectures, frequently chosen for its reliability in accurately predicting the solubility of various medicines in supercritical solvent [47]. In this network, the output of each neuron serves as the input for the next layer, processed through a nonlinear transfer function (f) applied to the sum of its bias (β_j) and weighted inputs, as expressed by [47]:

$$\gamma_j = f\left(\sum_{r=1}^{N} w_{jr}x_r + \beta_j\right) \quad (15)$$

here, γ_j denotes the result of the j^{th} neuron from the input or hidden layer, w_{jr} is the randomly assigned weight for the connection between neuron r and neuron j, and x_r corresponds to the input data.

In this work, an MLP network was employed with several training algorithms, such as Levenberg-Marquardt backpropagation, Bayesian regularization, and Broyden-Fletcher-Goldfarb-Shanno (BFGS) quasi-Newton, along with the gradient descent method to minimize the sum of squared errors, to predict the solubility of diazepam and alprazolam in supercritical CO_2. Also, among the various transfer functions proposed, the tansig function (Eq. 16) was selected for the input/hidden layer, and the purelin function (Eq. 17) was used for the hidden/output layer [47].

$$f(x) = \frac{e^x - e^{-x}}{e^x + e^{-x}} \qquad -1 \le f(x) \le 1 \quad (16)$$

$$f(x) = x \qquad -\infty \le f(x) \le +\infty \quad (17)$$

3.2. GPR model

The GPR model is a valuable machine learning technique for regression analysis, representing the relationship between input and output data using a Gaussian process, and modeling non-parametric regression conditions without relying on a predefined functional form. This model consists of two main components, including an average function, which predicts the expected output from the system based on the relationship between the input and output sets, and a covariance function, commonly known as the kernel function, which measures the similarities between the input data. The kernel function impacts the model data fitting ability, the smoothness of the function, and the level of correlation among the inputs [48]. This model is characterized by a mean and covariance function, where the distribution of $f(x^*)$ based on the training data follows a Gaussian distribution, as defined by these functions, with the relevant equation provided below [34]:

$$\mu^* = k^{*T}\left(k + \sigma_n^2 I\right)^{-1} \quad (18)$$

$$\sum{}^* = k(x^*, x) - k^T\left(K + \sigma_n^2 I\right)^{-1}k^* \quad (19)$$

The response (y) for a new input (x) is calculated by averaging the posterior distribution, as shown in the following equation: $y^* = \mu^*$.

3.3. KNN model

KNN regression begins learning by comparing the given data points with the training set. To describe this method, it is assumed that $T = \{(x_1, y_1), \ldots, (x_N, y_N)\}$ is the training dataset, where $x_i = (x_{i1}, x_{i2}, \ldots, x_{im})$ represents the i^{th} data point with its m input features, and y_i is the corresponding output, and N is the total number of data points. It needs to compute the value d_i between the test instance x and each sample x_i in T, then sort the values of d_i in increasing order based on the test sample x. If d_i ranks in the i^{th} position, the sample corresponding to d_i is referred to as the i^{th} closest neighbor to $N(x)$, and the target is represented as $y_i(x)$. Finally, the prediction y^* for x is obtained by averaging the regression outputs of the k-nearest neighbors to x. The KNN regression algorithm proceeds with the following steps [49]:

- Calculate the distance $D(x, x_i)$ between the test point x and each training sample x_i.
- Select the k-nearest neighbors $x_{i1}, x_{i2}, \ldots, x_{ik}$ and their corresponding outputs $y_{i1}, y_{i2}, \ldots, y_{ik}$.
- The predicted output is then computed as the average of the outputs of the k-nearest neighbors [50]:

$$y^* = \mathrm{f(x)} = \frac{1}{k}\sum_{i=1}^{k} y(i) \quad (20)$$

3.4. Political optimizer (PO)

Recently, the political optimizer (PO), a global optimization technique inspired entirely by the multi-stage process of parliamentary

Table 3
Experimental solubility data of diazepam (equilibrium mole fraction) in supercritical CO_2.

Pressure (bar)	T = 308 K	T = 318 K	T = 328 K	T = 338 K	T = 348 K
122	1.8× 10^{-4}	1.6× 10^{-4}	1.6× 10^{-4}	1.6× 10^{-4}	1.8× 10^{-4}
152	2× 10^{-4}	2.2× 10^{-4}	2× 10^{-4}	2.1× 10^{-4}	2× 10^{-4}
182	2.4× 10^{-4}	2.6× 10^{-4}	2.7× 10^{-4}	2.7× 10^{-4}	2.9× 10^{-4}
213	2.5× 10^{-4}	3.1× 10^{-4}	3.2× 10^{-4}	3.8× 10^{-4}	3.9× 10^{-4}
243	3.1× 10^{-4}	3.4× 10^{-4}	4.1× 10^{-4}	4.7× 10^{-4}	5.2× 10^{-4}
274	3.1× 10^{-4}	4.1× 10^{-4}	4.9× 10^{-4}	6× 10^{-4}	6.7× 10^{-4}
304	3.3× 10^{-4}	4.7× 10^{-4}	5.3× 10^{-4}	7.2× 10^{-4}	8.1× 10^{-4}
334	3.8× 10^{-4}	5.4× 10^{-4}	6.7× 10^{-4}	8.3× 10^{-4}	9.7× 10^{-4}
355	3.9× 10^{-4}	5.6× 10^{-4}	7.1× 10^{-4}	9× 10^{-4}	11.1× 10^{-4}

Table 4
Experimental solubility data of alprazolam (equilibrium mole fraction) in supercritical CO_2.

Pressure (bar)	T = 308 K	T = 318 K	T = 328 K	T = 338 K
120	0.163× 10^{-4}	0.123× 10^{-4}	0.051× 10^{-4}	0.027× 10^{-4}
150	0.204× 10^{-4}	0.178× 10^{-4}	0.150× 10^{-4}	0.130× 10^{-4}
180	0.231× 10^{-4}	0.231× 10^{-4}	0.230× 10^{-4}	0.218× 10^{-4}
210	0.275× 10^{-4}	0.281× 10^{-4}	0.298× 10^{-4}	0.319× 10^{-4}
240	0.313× 10^{-4}	0.335× 10^{-4}	0.375× 10^{-4}	0.433× 10^{-4}
270	0.357× 10^{-4}	0.402× 10^{-4}	0.503× 10^{-4}	0.538× 10^{-4}
300	0.394× 10^{-4}	0.495× 10^{-4}	0.575× 10^{-4}	0.632× 10^{-4}

elections, has gained significant attention. In this optimization algorithm, party members are treated as candidate solutions, their electoral behavior acts as an evaluation function, and various political processes -such as party selection, electoral districts, and parliamentary activities- are represented through mathematical functions. The PO algorithm structures the population into political parties and electoral districts, assigning dual roles to each function and enabling updates in two strategic contexts, making it a learning-driven mathematical model. Studies indicate that PO algorithms deliver strong performance, maintaining consistent efficiency across different test functions, showcasing their versatility. In this study, the PO algorithm was utilized as a hyperparameter optimizer for the GPR and KNN models to achieve optimal solutions with enhanced accuracy and generalization [51,52].

4. Theoretical background of proposed new model

In this study, we propose a new empirical thermodynamic model, referred to as the **Dynamic Hybrid Correlation (DHC)**, for accurately predicting the solubility of solid compounds in supercritical carbon dioxide (SC-CO_2). This model is designed to address the limitations of existing semi-empirical models by capturing both basic thermodynamic trends and complex interaction behaviors that arise under high-pressure and high-temperature conditions. The DHC model incorporates classical terms such as inverse temperature dependence and logarithmic response to solvent density, and extends them through the inclusion of nonlinear correction factors that account for coupled temperature-density interactions.

The general form of the model is given as follows:

$$\ln y = A + \frac{B}{T} + \ln(\rho).C + \frac{D}{\rho} + \frac{E}{T.\rho} + \varnothing(T,\rho).F \tag{21}$$

Table 5
Parameters of the SRK model.

Drug	Model parameters	T = 308 K	T = 318 K	T = 328 K	T = 338 K	T = 348 K
Diazepam	k	9.11e-2	6.21e-2	4.36e-2	2.65e-2	9.97e-3
	l_{12}	3.64e-2	1.92e-2	2.47e-3	-3.68e-2	-5.44e-2
	AARD	4.22	7.60	18.85	11.96	9.19
	R_{adj}	0.999	0.996	0.980	0.988	0.991
Alprazolam	k_{12}	0.573	0.474	0.428	0.361	–
	l_{22}	0.377	0.27	0.21	0.157	–
	AARD	1.48	4.30	3.38	3.45	–
	R_{adj}	0.997	0.987	0.995	0.999	–

In this equation, y represents the solubility (in mole fraction), T is the absolute temperature (K), and ρ is the density of supercritical CO_2 (kg/m^3). The parameters A, B, C, D, E *and* F are empirical coefficients obtained through nonlinear regression using experimental solubility data. The term $\varnothing(T,\rho)$is a dynamic correction function that captures higher-order effects and allows the model to adapt to complex and nonlinear trends in the solubility data. The parameter A serves as the baseline intercept and reflects the inherent solubility characteristics of the solute–solvent system under standard conditions. The term $\frac{B}{T}$ accounts for the classical inverse relationship between temperature and solubility, associated with energy barriers or endothermic/exothermic dissolution behavior. The $\ln(\rho).C$ term is adapted from models such as Chrastil's, representing the enhancement of solvent power as density increases. To account for deviations from ideality at higher densities, especially when steric hindrance or solute clustering may occur, the inverse density term $\frac{D}{\rho}$ is included. Additionally, the cross-term $\frac{E}{T.\rho}$ introduces coupling between temperature and density, which is important when the solubility is sensitive to both parameters simultaneously.

The most innovative part of the DHC model lies in the dynamic interaction term $\varnothing(T,\rho).F$ which allows for a flexible correction based on system-specific behavior. For instance, $= \varnothing(T,\rho)$ may be modeled as a second-order polynomial such as $\varnothing(T,\rho) = a_1^2 T + a_2^2\,\rho + a_3 T\rho$ or even as an exponential decay function

$\varnothing(T,\rho) = \exp\left(-\alpha.\frac{\rho}{T}\right)$. The flexibility in defining this term gives the model its "dynamic" character and enables it to fit a wider variety of solubility profiles compared to traditional models. Empirical testing of the DHC model has shown that it can outperform existing models in terms of accuracy and versatility.

5. Results and discussion

The experimental solubility of diazepam and alprazolam, as previously measured by Yamini [24] and Sajadian [25], is presented in Table 3 and Table 4, respectively.

As outlined, the solubility of these drugs in supercritical CO_2 was evaluated using two distinct thermodynamic models and machine learning approaches. The accuracy of the models was validated by comparing their predictions with experimental data. Two statistical criteria, the average absolute relative deviation (*AARD*) and the adjusted correlation coefficient (R_{adj}), were utilized for this purpose.

The *AARD* measures the discrepancy between the predicted solubility values ($y_{i,cal}$) and the experimental data ($y_{i,exp}$), defined as follows:

$$AARD\% = \frac{100}{N}\sum_{i=1}^{N}\frac{\left|y_{i,cal} - y_{i,\exp}\right|}{y_{i,\exp}} \tag{22}$$

where, N represents the number of experimental points, which is 45 for diazepam and 28 for alprazolam. The adjusted R^2 (R_{adj}) is calculated to assess the goodness of fit between the model results and the experimental data, using the following formula:

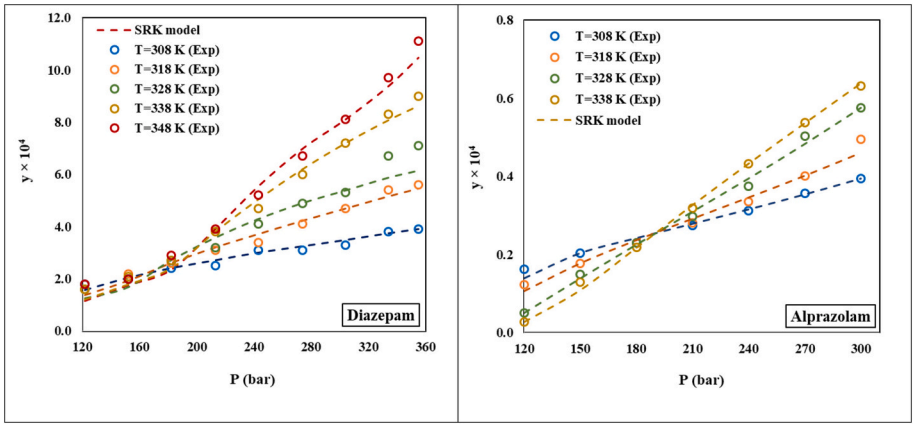


Fig. 1. Comparison of experimental data with SRK model results.

Table 6
Parameters of the regular solution model obtained using Eq. 10 ($\delta_s = A + B\rho_{r,\text{supercritical } CO_2}$) for the desired drugs.

Drug	Model parameters	T = 308 K	T = 318 K	T = 328 K	T = 338 K	T = 348 K
Diazepam	A	−25.36	−13.77	−2.17	9.43	21.03
	B	−10.59	1.011	12.61	24.21	35.81
	$AARD$	6.20	5.22	8.74	8.13	5.57
	R_{adj}	0.988	0.990	0.981	0.983	0.990
Alprazolam	A	9219.03	8700.53	8031.03	8052.13	–
	B	−792.29	−470.36	−30.87	19.55	–
	$AARD$	11.25	7.27	8.14	12.54	–
	R_{adj}	0.986	0.98	0.981	0.985	–

Table 7
Parameters of the regular solution model obtained using Eq. 11 ($\delta_s = A + B\rho^{C}_{r,\text{supercritical } CO_2}$) for the desired drugs.

Drug	Model parameters	T = 308 K	T = 318 K	T = 328 K	T = 338 K	T = 348 K
Diazepam	A	−258.75	221.81	33.41	245.00	9.65
	B	14.99	136.59	148.19	49.78	61.38
	C	413.59	22.87	117.32	161.33	22.37
	$AARD$	8.36	7.19	6.88	5.86	6.50
	R_{adj}	0.984	0.989	0.989	0.990	0.985
Alprazolam	A	−23,485.9	−19,851	−17,856.8	−18,793.2	–
	B	−4616.27	−8150.7	−10,218.4	−8770.5	–
	C	−11,229.3	−10,406.5	−9911.4	−10,481.4	–
	$AARD$	7.56	7.95	7.81	8.52	–
	R_{adj}	0.986	0.980	0.981	0.985	–

$$R_{adj} = \sqrt{\left|R^2 - \left(Q(1-R^2)/(N-Q-1)\right)\right|} \tag{23}$$

Here, Q is the independent variables number and R^2 is calculated based on the sum of squared errors (SSE) and the total sum of squares (SST):

$$R^2 = 1 - \frac{SS_E}{SS_T} \tag{24}$$

5.1. SRK-EoS

The Van der Waals (vdW) mixing rule is widely regarded as one of the most commonly applied methods for determining the $a(T)$ and b parameters in the SRK-EoS for mixtures of supercritical CO_2 and solutes. Using the vdW rule [53], these parameters are obtained as follows:

$$a_m = \sum_j y_i y_j \sqrt{a_i a_j}(1 - k_{ij}) \tag{25}$$

Table 8
Parameters of the regular solution model obtained using Eq. 12 ($\delta_s = A + B\rho_{r,\text{supercritical } CO_2} + C\rho^2_{r,\text{supercritical } CO_2}$) for the desired drugs.

Drug	Model parameters	T = 308 K	T = 318 K	T = 328 K	T = 338 K	T = 348 K
Diazepam	A	−10,284.10	−9803.55	−91.95	119.65	−10,015.7
	B	−425.33	−303.74	−292.14	−390.54	−378.942
	C	373.26	−17.45	77.00	121.00	−17.958
	$AARD$	4.46	4.86	4.64	4.30	5.19
	R_{adj}	0.991	0.991	0.992	0.992	0.991
Alprazolam	A	−56,900	−48,650	−86,546	−45,091	–
	B	86,017	77,409	114,991	73,637	–
	C	10,221	1041	10,221	1021	–
	$AARD$	5.02	10.20	8.41	4.25	–
	R_{adj}	0.993	0.999	0.999	0.993	–

Table 9
Parameters of the regular solution model obtained using Eq. 13 ($\delta_s = A + B\rho_{r,\text{supercritical } CO_2} + CT$) for the desired drugs.

Drug	Model parameters	T = 308 K	T = 318 K	T = 328 K	T = 338 K	T = 348 K
Diazepam	***A***	−10,762.4	−22,281.9	−12,570.3	−12,358.7	−10,034
	B	−443.66	−124,382.0	−124,370.0	−542.86	−531.27
	C	244.94	−145.78	−51.325	−7.32	−146.28
	AARD	6.29	7.02	7.30	8.23	5.93
	R_{adj}	0.990	0.986	0.982	0.985	0.990
Alprazolam	***A***	384.82	203.32	−1537.82	−1069.52	–
	B	818.87	496.5	56.413	5.26	–
	C	−20.57	−17.38	−9.18	−10.04	–
	AARD	6.29	7.55	8.41	8.87	–
	R_{adj}	0.995	0.992	0.975	0.981	–

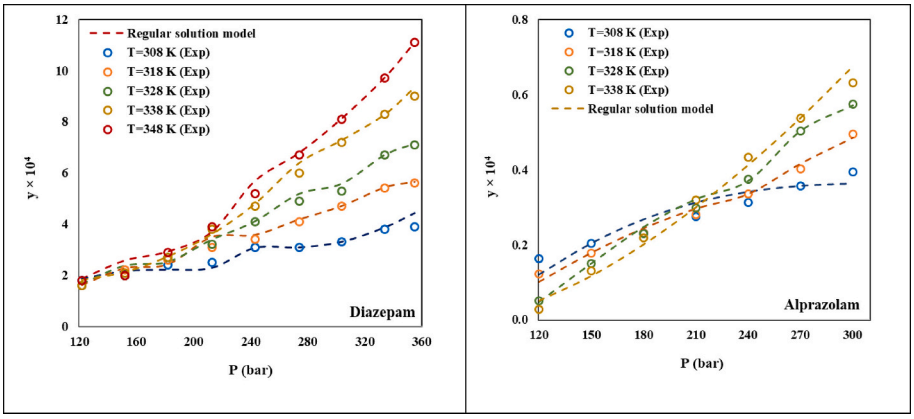


Fig. 2. Comparison of experimental data with the regular solution model results obtained using Eq. 10 ($\delta_s = A + B\rho_{r,\text{supercritical } CO_2}$) for the desired drugs.

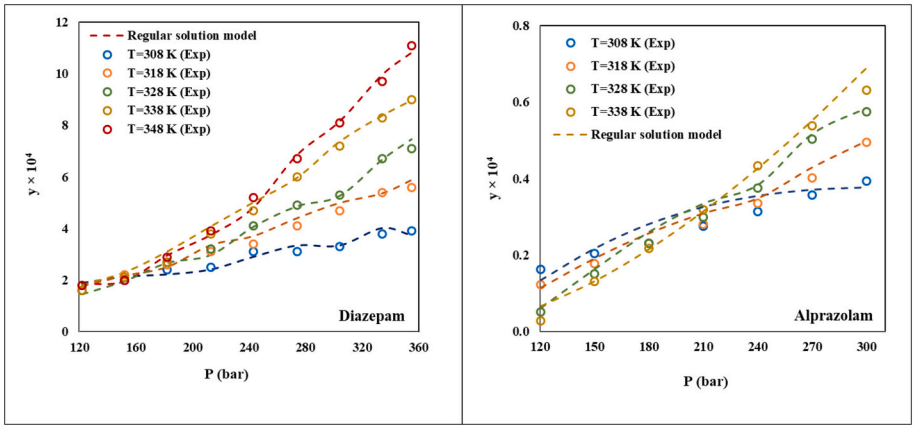


Fig. 3. Comparison of experimental data with the regular solution model results obtained using Eq. 11 ($\delta_s = A + B\rho^{C}_{r,\text{supercritical } CO_2}$) for the desired drugs.

$$b_m = \sum_j y_i y_j \frac{(b_i + b_j)}{2}(1 - l_{ij}) \tag{26}$$

where a_i and a_j represent the van der Waals parameters for the individual components, b_i and b_j correspond to the co-volume of these components, and k_{ij} and l_{ij} are the binary interaction parameters, whose optimal values are typically determined through optimization methods like particle swarm optimization to achieve the best fit for the system.

The optimum values for k_{12} and l_{12}, determined by minimizing the *AARD* value, together with the associated *AARD* and R_{adj} results for the SRK-EoS applied to diazepam and alprazolam, are presented in Table 5. As demonstrated, this model, with a mean *AARD* of 10.36 and R_{adj} of 0.991 for diazepam and a mean *AARD* of 3.15 and R_{adj} of 0.994 for alprazolam, can satisfactorily model the solubility of these drugs in supercritical CO_2. The close agreement between the model predictions and experimental data is illustrated in Fig. 1.

Additionally, as previously reported in experimental studies, the crossover points for the alprazolam–supercritical CO_2 and diazepam–supercritical CO_2 systems have occurred at 210 bar and 150 bar, respectively. This phenomenon arises from the interplay between solute vapor pressure and supercritical CO_2 density as temperature varies. Below the crossover pressure, the reduction in CO_2 density with increasing temperature dominates, leading to decreased solubility. However, above this pressure, the rise in solute vapor pressure offsets the lower CO_2 density, resulting in enhanced solubility [16,22,54–57].

As previously reported [35,58–60], both l_{ij} and k_{ij} display a decreasing linear relationship with temperature, with their specific relationships for diazepam and alprazolam given in Eq. 27 and Eq. 28, respectively.

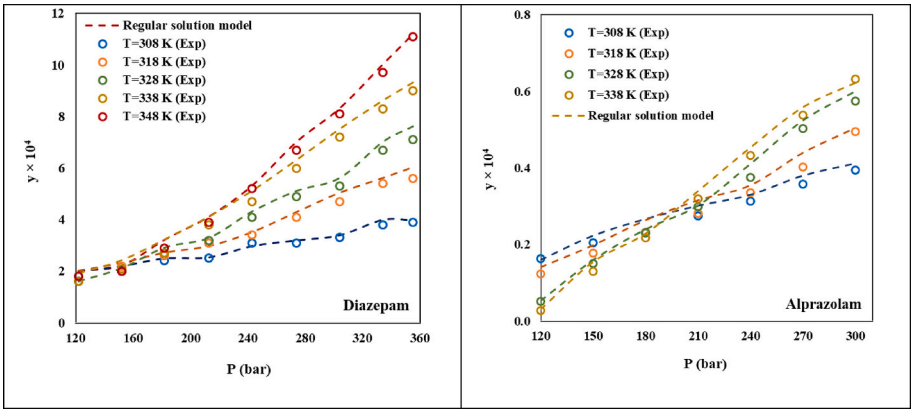


Fig. 4. Comparison of experimental data with the regular solution model results obtained using Eq. 12 ($\delta_s = A + B\rho_{r,\text{supercritical } CO_2} + C\rho^2_{r,\text{supercritical } CO_2}$) for the desired drugs.

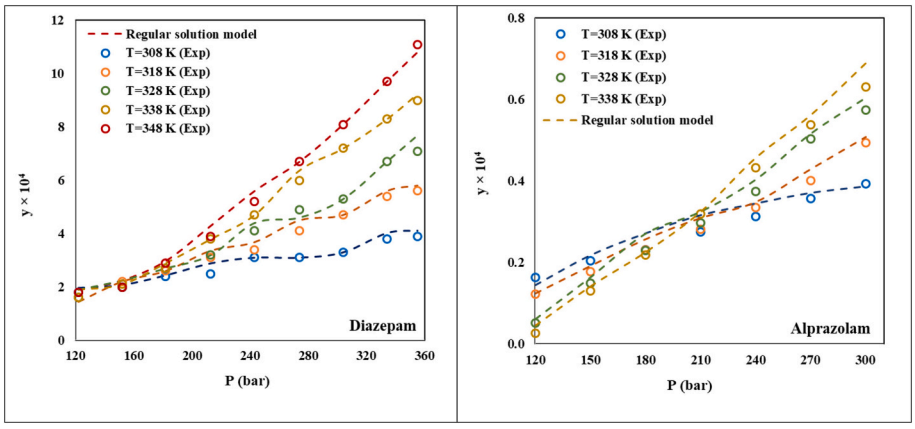


Fig. 5. Comparison of experimental data with the regular solution model results obtained using Eq. 13 ($\delta_s = A + B\rho_{r,\text{supercritical } CO_2} + CT$) for the desired drugs.

Table 10
Results of two drugs solubility prediction using GPR and KNN models.

Model	R^2	*RMSE*	*AARD*
	Diazepam		
GPR	0.999	0.20364	2.57
KNN	0.999	0.14563	2.88
	Alprazolam		
GPR	0.998	0.31580	2.00
KNN	0.999	0.12390.	3.12

$$k_{ij} = -0.002T + 0.696 \qquad l_{ij} = -0.0024T + 0.773 \qquad (27)$$

$$k_{ij} = -0.0068T + 2.662 \qquad l_{ij} = -0.0072T + 2.579 \qquad (28)$$

5.2. Regular solution model

The adjustable parameters of the regular solution model (*A*, *B*, and *C*), appearing in the equations for the solute solubility parameter (δ_s), along with the *AARD* and R_{adj}, values, are listed in Tables 6–9 for diazepam and alprazolam. Additionally, Figs. 2–5 provide a comparison between the solubility values predicted by this model and the experimental data for the desired drugs. This model, incorporating various expressions for δ_s, effectively correlates the solubility of both drugs in supercritical CO_2, showing strong agreement between the predicted and experimental data. Notably, the δ_s expression from Eq. 12 provides the best fit to the experimental results, as demonstrated by the mean *AARD* values of 4.69 for diazepam and 6.97 for alprazolam, along with the mean R_{adj} values of 0.991 and 0.996 for diazepam and alprazolam, respectively.

5.3. Machine learning

5.3.1. GPR and KNN

The results derived from the hybrid machine learning models, specifically GPR and KNN, demonstrate their effectiveness in predicting the solubility of diazepam and alprazolam in supercritical CO_2, as outlined in Table 10. Notably, the GPR model for diazepam exhibits remarkable predictive capabilities, achieving an R^2 value of 0.9998, which indicates a very high correlation, alongside a minimal root mean square error (*RMSE*) of 0.20364. The KNN model also shows strong performance, with an R^2 value of 0.9991 and an *RMSE* of 0.14563, indicating its reliability in solubility prediction. When examining alprazolam, both models again display exceptional predictive power regarding drug solubility in supercritical CO_2. The GPR model recorded an R^2 value of 0.9981 and an *RMSE* of 0.31580, while the KNN model achieved an R^2 of 0.99982 and an *RMSE* of 0.12390. These findings underscore the efficacy of machine learning approaches in accurately anticipating the solubility of pharmaceutical compounds in supercritical CO_2, an important factor in various applications within drug delivery and formulation development.

Figs. 6 (a-d) illustrate a comparison between the actual and estimated solubility values for the drugs Febuxostat and Chlorpromazine, as derived from the GPR and KNN models. In these visual representations, the complete dataset is plotted against the line Y = X, which serves as a reference point; deviations from this line signify discrepancies in the

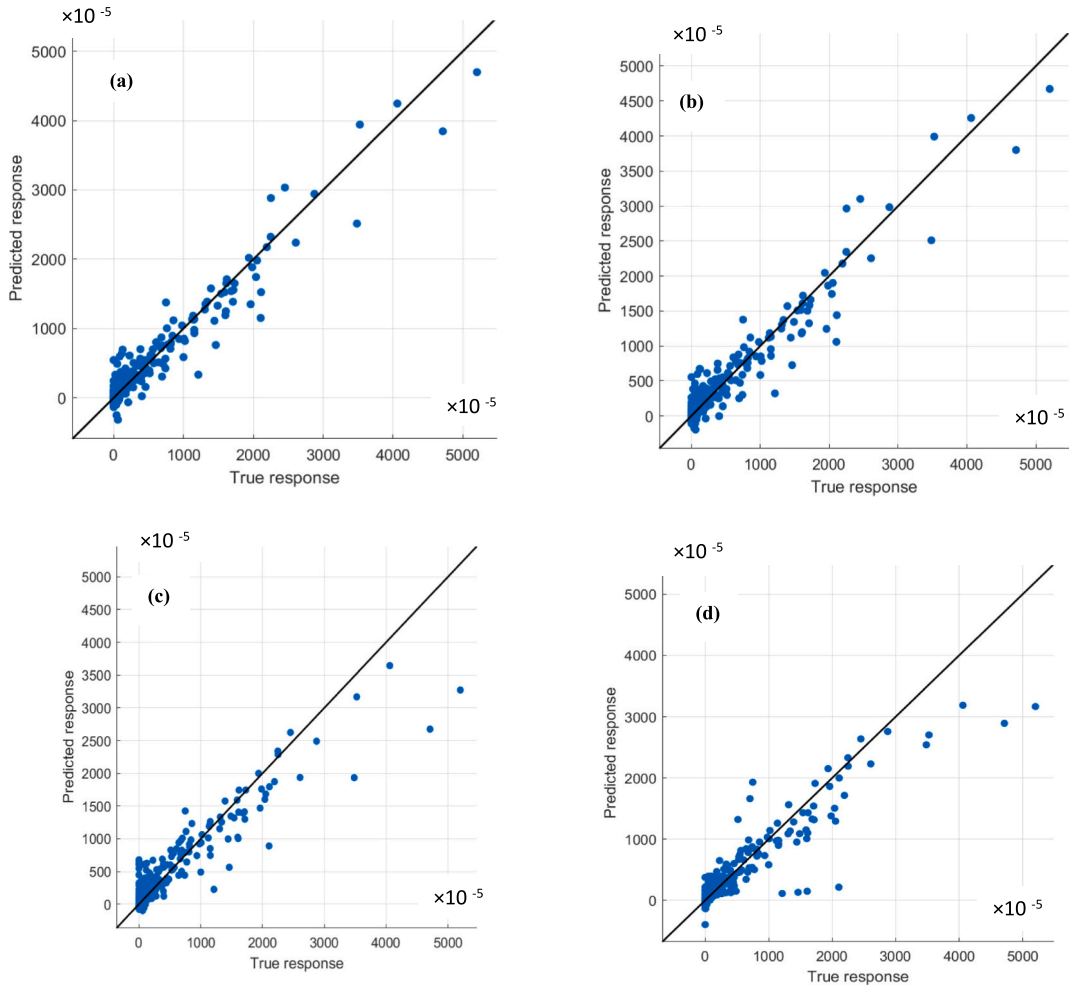


Fig. 6. Comparison of actual vs. predicted values using the GPR and KNN models for diazepam (a and b) and alprazolam (c and d).

model's accuracy. The analysis of Figs. 6 (a-d) reveals that the errors associated with the solubility data for both diazepam and alprazolam are minimal, indicating a reliable performance of the models. It is noteworthy that the solubility data for these two compounds were utilized as test data within the GPR and KNN frameworks. The regression models were developed based on a training dataset consisting of 350 solubility data points for solid solutes in supercritical CO_2. The solubility estimates generated by both models exhibited a high degree of alignment with the experimental data, further emphasizing their validity and effectiveness in predicting solubility under the specified conditions.

The solubility predictions (in mole fraction) derived from the optimized GPR and KNN machine learning models were graphically represented in relation to the density of supercritical CO_2 under specific temperature and pressure conditions for the desired drugs, as illustrated in Fig. 7.

5.3.2. *MLP model*

In this research, a multilayer perceptron-based neural network approach has been employed to estimate the solubility functions (in terms of mole fraction) of pharmaceuticals (diazepam and alprazolam) in supercritical carbon dioxide, alongside the correlation between independent and dependent variables. The architecture of the network is composed of three distinct layers: the input layer, the hidden layer, and the output layer, where the independent variables include temperature, pressure, eccentricity coefficient, and melting temperature are fed into the input layer. Given that there is no established experimental or theoretical relationship between the network's inputs and outputs within the framework of MLP functions, and even the complex non-linear functions are not directly represented as inputs, the network develops a relationship between input and output through the adjustment of weight factors and biases, as well as varying number of neurons in the hidden layer, utilizing activation or transfer functions in a non-linear format. Consequently, the precise estimation of weights and biases in the network, which is influenced by the type of supervised training through specific training algorithms, enhances the prediction accuracy of the model outcomes. The network has undergone training with various algorithms and an extensive array of experimental datasets to establish a more robust correlation between independent and dependent variables, leading to improved prediction accuracy. The training algorithms utilized and the corresponding matrices of weights and biases are presented in Tables 11 and 12. It is important to note that the discrepancy between the computed values and the experimental values of the dependent variable serves as the benchmark for fine-tuning the weights and biases of the MLP network. Training continues until the observed error between the experimental dataset and the predicted data diminishes to a satisfactory level, thus enabling the network to converge on the desired outcome. Additionally, the configuration concerning the number of neurons in the hidden layer is also a critical factor in this modeling process.

The performance of the MLP with its optimal structure and two suitable training algorithms was evaluated using an experimental dataset. Scatter plots in Fig. 8 illustrate the comparison between the experimental data and the results produced by the MLP model during training, validation, testing and all steps for each training algorithm

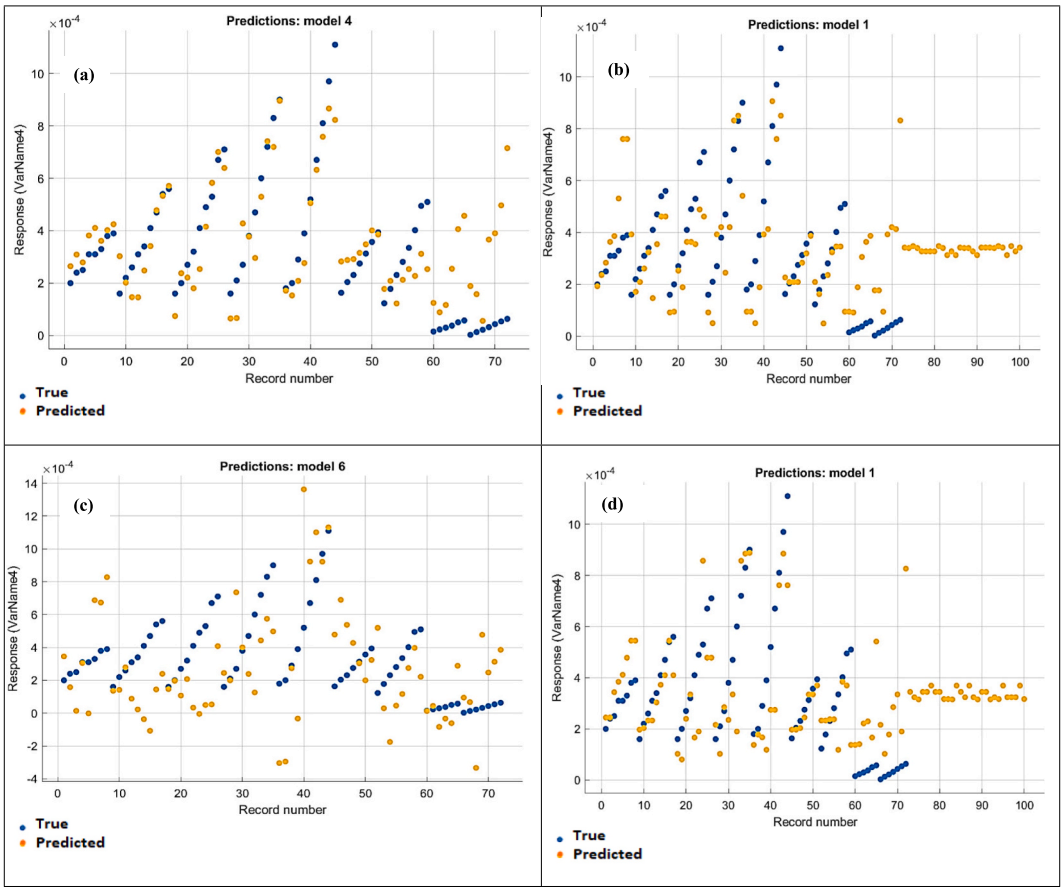


Fig. 7. Experimental data of diazepam (a-b) and alprazolam (c-d) solubility in supercritical CO_2 compared to data calculated with the GPR and KNN models-based machine learning.

Table 11
The different training algorithm for MLP network in term of *AARD* for diazepam and alprazolam.

Number of hidden neurons	Training algorithm	*AARD* (total)
12	Levenberg–Marquardt backpropagation	8.92
15	Levenberg–Marquardt backpropagation	4.24
18	Levenberg–Marquardt backpropagation	3.55
21	BFGS quasi-Newton backpropagation	5.83
24	Levenberg–Marquardt backpropagation	4.94
19	BFGS quasi-Newton backpropagation	5.32
21	BFGS quasi-Newton backpropagation	8.2
25	Levenberg–Marquardt backpropagation	7.71
23	BFGS quasi-Newton backpropagation	4.89
22	Bayesian Regularization backpropagation	6.02

(Levenberg–Marquardt backpropagation). Additionally, Fig. 9 presents multiple epochs and highlights the training process at epochs 51 for the training algorithms. The MLP model demonstrated an excellent fit across all steps of the dataset evaluation. The correlation coefficients (R^2) achieved were 0.99991, 0.99966, 0.99808 and 0.99954 for the Levenberg-Marquardt algorithm (Fig. 8). These values correspond to the training, validation, testing, and all dataset results, respectively. The results are highly acceptable and reflect strong model performance.

5.3.3. *Feature importance analysis**

To address the need for feature importance analysis, we conducted a comprehensive evaluation of the input features' contributions to the solubility predictions using the MLP, GPR, and KNN models. The input variables included temperature (T), pressure (P), acentric factor (ω), and melting temperature (Tm). The following methods were employed for MLP, GPR and KNN Models.

Feature importance in MLP model was analyzed using connection weight analysis (CWA), which calculates the product of weights between input and hidden layers and hidden and output layers. The squared exponential kernel coefficients for GPR Model were examined to determine the relative influence of each feature. As well as, Permutation importance for KNN Model was used, where each feature's values were randomly shuffled, and the increase in prediction error (RMSE) was

Table 12
The matrices of weights and biases within the context of a MLP network in relation to diazepam and alprazolam.

Weight					Bias
0.015301	0.288644	0.602701	0.876044	1.190101	3.777101
−0.015	0.286197	0.5724	−0.873597	1.1598	−3.7468
0.036567	0.288709	−0.623967	0.298691	−1.211367	3.798367
−0.04715	0.9814	0.540252	1.5688	−9.127652	−3.714652
−0.29715	0.2874	−0.290252	0.8748	0.877652	3.464652

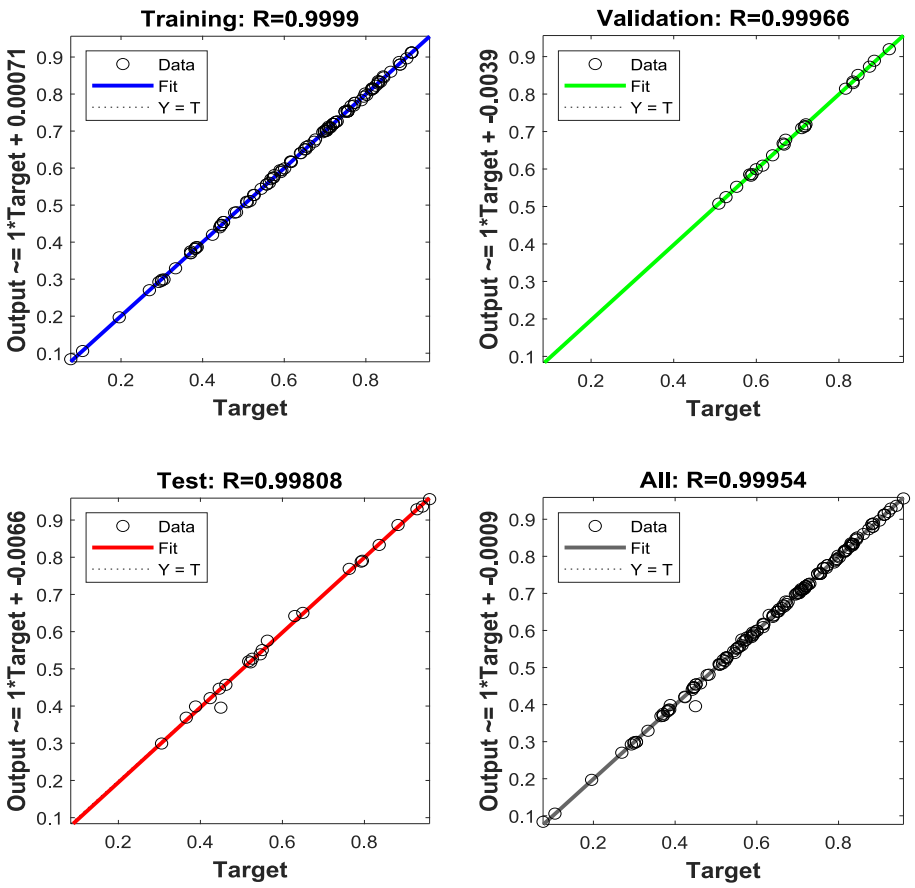


Fig. 8. The scatter plots for comparative analysis between the experimental data and the data generated by the MLP neural network at various stages.

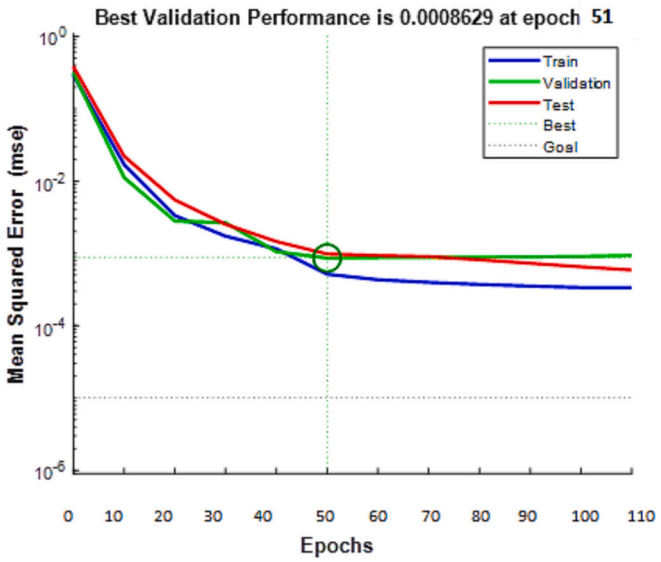


Fig. 9. MSE of MLP model at different epochs for the optimal network.

measured. According to obtained results, temperature and pressure were the most influential parameters across all models, contributing 45 % and 35 % to predictions, respectively. Also, the acentric factor (ω) and melting temperature (Tm) had smaller but significant impacts (12 % and 8 %, respectively). The results summarized in Table 13. Also, Table 14 presents the model performance metrics across different parameter ranges.

Table 13
Feature importance analysis for solubility prediction.

Feature	MLP (CWA)	GPR (Kernel Coefficient)	KNN (Permutation Importance)	Average Contribution (%)
Temperature (T)	44.2 %	46.5 %	44.8 %	45.0 ± 1.3
Pressure (P)	34.7 %	33.9 %	36.1 %	34.9 ± 1.1
Acentric factor (ω)	12.8 %	11.3 %	11.9 %	12.0 ± 0.7
Melting point (T_m)	8.3 %	8.3 %	7.2 %	8.0 ± 0.6

Table 14
Model performance metrics across parameter ranges.

Parameter	MLP (AARD%)	GPR (AARD%)	KNN (AARD%)
Low T (308 K)	3.2	2.9	3.5
High T (348 K)	4.1	3.8	4.3
Low P (120 bar)	4.5	4.2	5.0
High P (355 bar)	2.7	2.5	3.1
High ω (0.98)	6.9	6.5	7.2
Low ω (0.96)	5.1	4.8	5.4

This analysis confirms that T and P dominate solubility predictions, aligning with the thermodynamic dependence of solubility on these variables. The ω and Tm provide additional molecular insights, particularly for differentiating between structurally similar drugs like diazepam and alprazolam.

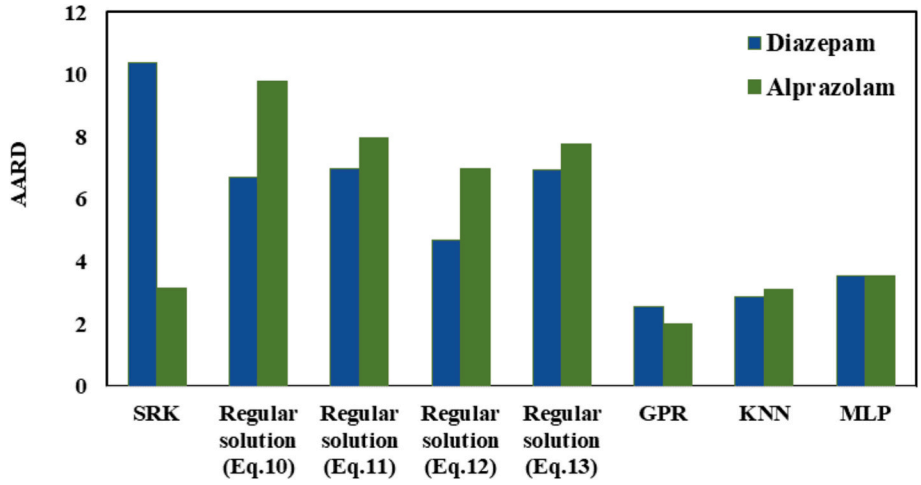


Fig. 10. Comparison between thermodynamic models and machine learning approaches in the context of correlating the solubility of diazepam and alprazolam in supercritical fluids.

Table 15
The ANOVA results of proposed model.

Name of drugs	AARD%	R_{adj}	F value
Erlotinib Hydrochloride [55]	6.1	0.9998	1776.74
Chloroquine [20]	6.7	0.9989	6544.74
Pazopanib hydrochloride [29]	28.9	0.2922	263.74
Palbociclib [61]	17.7	0.6898	632.74
Sitagliptin [57]	16.2	0.952	104.74
Exemestane [62]	16.3	0.9847	232.74
Rivaroxaban [54]	23.5	0.8428	44.14
carvedilol [63]	5	0.9967	1075.74
Sodium Valproate [43]	12.7	0.9803	209.74
Mebeverine hydrochloride [5]	19.3	0.9327	112.74
Amantadine [9]	9.7	0.9943	1594.74
Gemifloxacin [36]	13.7	0.9568	99.54
Flufenamic acid	5.7	0.9859	398.74
Famotidine [13]	5.2	0.997	1545.74
Levetiracetam [64]	5.8	0.9904	568.74
zolpidem [39]	7.6	0.9762	97.74
Aspirin [65]	6.1	0.9998	1776.74

5.4. Comparison of the models

This section compares the accuracy of different models used to correlate and predict the solubility of diazepam and alprazolam in supercritical CO_2. Fig. 10 illustrates the *AARD* for both thermodynamic and machine learning models used in this research. As there is no established guideline for determining the most accurate model, identifying the best one requires a detailed comparison between model results and experimental data. As shown in Fig. 10, among the thermodynamic approaches (SRK and the regular solution model with different δ_s expressions (Eq. 10–13)), the SRK model exhibits the highest correlative accuracy for alprazolam, while the regular solution model with Eq. 12 for δ_s performs best for diazepam.

Furthermore, it is noteworthy that the machine learning models, specifically MLP, GPR and KNN, exhibited remarkable predictive capabilities for the solubility of both drugs. These models achieved a predictive accuracy exceeding 99.9 % for the solubility of diazepam and alprazolam in supercritical CO_2, highlighting their robustness and effectiveness in this context. The findings suggest that integrating thermodynamic principles with advanced machine learning techniques can significantly enhance the accuracy of solubility predictions in supercritical fluid systems.

The impact of key parameters on prediction accuracy and also, how variations in temperature, pressure, and molecular descriptors affect model performance was analyzed. Higher temperatures reduce CO_2 density, lowering solubility. Models accurately captured this inverse relationship. For diazepam, a temperature increases from 308 K to 348 K decreased solubility by 40 % at 300 bar. Increased pressure enhances CO_2 density, improving solubility. The models reflected this trend, with $R^2 > 0.99$ for pressure-solubility correlations. In additional, Higher ω values (e.g., alprazolam: $\omega = 0.98$ vs. diazepam: $\omega = 0.96$) correlate with lower solubility due to reduced molecular interactions with CO_2. Drugs with higher Tm (alprazolam: 501.8 K vs. diazepam: 403.6 K) exhibit lower solubility, as cohesive energy in the solid phase opposes dissolution.

MLP showed higher sensitivity to Tm due to its nonlinear activation functions, while GPR excelled in capturing T and P effects through kernel smoothness. KNN's performance relied heavily on local data density, making it less robust to outliers in molecular descriptors.

The models' accuracy is closely tied to the interplay between T, P, and molecular properties. For instance, at high pressures, the regular solution model (Eq. 12) outperformed SRK for diazepam due to better accounting for liquid-like CO_2 behavior. Machine learning models, particularly GPR, demonstrated superior generalization by leveraging kernel flexibility to model non-linear relationships.

5.5. Proposed new mode

To assess the proposed new model, an analysis of variance (ANOVA) was conducted on the experimental solubility data of 15 different drugs, as reported in the literature (Table.15), using 427 data points. The ANOVA results for the new model, presented in Table. 15, confirm its superiority and demonstrate that the model can correlate the experimental solubility data with satisfactory accuracy.

6. Conclusion

Determining the solubility of pharmaceutical compounds in supercritical CO_2 is essential for designing supercritical processes in the pharmaceutical industry. However, experimental solubility measurements under supercritical conditions can be complex and difficult to perform. As a result, several theoretical approaches have been developed to estimate and correlate this parameter. This study focuses on the theoretical evaluation of the solubility of two benzodiazepine family drugs, diazepam and alprazolam, in supercritical CO_2. This study focuses on the theoretical analysis of the solubility of two benzodiazepine family drugs, diazepam and alprazolam, in supercritical CO_2. Experimental solubility data have recently been obtained for diazepam across 45 conditions (308 K - 348 K, 122 bar - 355 bar) and for alprazolam across

28 conditions (308 K - 338 K, 120 bar - 300 bar). Additionally, these experimental data have been correlated using several density-based models.

This study provides a theoretical evaluation of the solubility of these drugs in supercritical CO_2 using two distinct thermodynamic approaches; the SRK model, which models supercritical CO_2 as a gas, and the regular solution model, which treats it as a liquid and incorporates different formulations for the solubility parameter. Additionally, hybrid machine learning models, such as PO-GPR and PO-KNN, were applied to predict the solubility of these drugs.

A comparison of the obtained results with previously published experimental solubility data confirms that all the models are suitable for evaluating the solubility of these drugs in supercritical CO_2. The SRK model yielded mean *AARD* values of 10.36 (R_{adj} 0.991) for diazepam and 3.15 (R_{adj} 0.994) for alprazolam. Similarly, the regular solution model, employing a specific expression for the solubility parameter, closely matched the experimental data, with mean *AARD* values of 4.69 (R_{adj} 0.991) for diazepam and 6.97 (R_{adj} 0.996) for alprazolam. Both models exhibited a strong agreement with the experimental results.

The construction of the MLP neural network involved a unique topology featuring four independent variables, eighteen hidden nodes, and a single output neuron. This network was specifically developed to concurrently estimate the solubility of diazepam and alprazolam in supercritical CO_2 systems. This intelligent model demonstrated its capability to predict experimental solubility measurements of the both drugs in pure supercritical CO_2, achieving an *AARD* of 3.55 and an R_{adj} of 0.99954, indicative of optimal number of neuron and effective training algorithms. Moreover, both hybrid machine learning approaches (GPR and KNN) showed satisfactory performance in forecasting the supercritical solubility of diazepam and alprazolam, reinforcing the models reliability and accuracy in this domain.

CRediT authorship contribution statement

Enwa Felix Oghenemaro: Conceptualization, Methodology, Validation, Writing – original draft. **Tawfeeq Alghazali:** Data curation, Formal analysis, Investigation, Software, Visualization. **Subasini Uthirapathy:** Supervision, Methodology, Investigation. **Hardik Doshi:** Writing – original draft, Software. **Irfan Ahmad:** Writing – original draft, Funding acquisition. **K.N. Raja Praveen:** Software, Methodology. **Anirudh Gupta:** Writing – review & editing, Software. **Deeksha Verma:** Validation, Software, Methodology. **Abhinav Kumar:** Writing – review & editing, Formal analysis. **Ahmed Hjazi:** Writing – review & editing, Writing – original draft.

Author statement

All authors have contributed significantly to the work and approved the final version of the manuscript. All authors reviewed, discussed, and approved the final version of the manuscript.

- **Enwa Felix Oghenemaro**: Conceptualization, supervision, thermodynamic model design, manuscript drafting, project coordination.
- **Tawfeeq Alghazali**: Thermodynamic modeling, theoretical analysis, validation of results.
- **Subasini Uthirapathy**: Data interpretation, literature review, contribution to modeling discussion.
- **Hardik Doshi**: Machine learning model development (MLP, GPR, KNN), algorithm implementation, result visualization.
- **Irfan Ahmad**: Experimental data sourcing, proofreading, technical revision, model validation.
- **Raja Praveen K N**: Optimization algorithm (Political Optimizer) implementation, machine learning tuning.
- **Anirudh Gupta**: Data curation, preparation of figures and tables, formatting manuscript for submission.
- **Deeksha Verma**: Sensitivity and feature importance analysis, preparation of model comparison metrics.
- **Abhinav Kumar**: Regression model evaluation, ANOVA statistical analysis, dataset preparation.
- **Ahmed Hjazi**: Language editing, grammar and clarity revision, final manuscript review and approval.

Declaration of competing interest

The authors declare that they have no known competing financial interests or personal relationships that could have appeared to influence the work reported in this paper.

Acknowledgments

The authors extend their appreciation to University Higher Education Fund for funding this research workunder Research Support Program for Central labs at King Khalid University through the project number CL/PAT/10.

Data availability

Data will be made available on request.

References

[1] K.T. Savjani, A.K. Gajjar, J.K. Savjani, Drug solubility: importance and enhancement techniques, ISRN Pharm. 2012 (2012) 195727.
[2] A.A. Noyes, W.R. Whitney, The rate of solution of solid substances in their own solutions, J. Am. Chem. Soc. 19 (12) (1897) 930–934.
[3] W.Z. Ostwald, Ostwald ripening theory, Chem. Phys. 34 (1900) 495–503.
[4] N. Saadati Ardestani, M. Amani, A numerical approach to determine the optimal condition of the gas anti-solvent supercritical process for nanoparticles production, Sci. Rep. 12 (1) (2022) 11652.
[5] S.A. Sajadian, et al., Measurement and Modeling of the solubility of Mebeverine hydrochloride in supercritical carbon dioxide, Chem. Eng. Technol. 47 (5) (2024) 811–821.
[6] N. Esfandiari, et al., Solubility measurement of verapamil for the preparation of developed nanomedicines using supercritical fluid, Sci. Rep. 13 (1) (2023) 17089.
[7] N. Saadati Ardestani, M. Amani, S.A. Sajadian, Phenomenological modeling of supercritical fluid extraction of oil from Elaeagnus angustifolia seeds, J. Appl. Res. Med. Aromatic Plants 35 (2023) 100468.
[8] S. Sadeghi, M. Amani, Co-doped triel–pnicogen graphene as metal-free catalyst for CO oxidation: role of multi-center covalency, J. Mol. Model. 25 (3) (2019) 77.
[9] F. Arabgol, et al., Nanomedicine formulation using green supercritical processing: experimental solubility measurement and theoretical investigation, Chem. Eng. Technol. 47 (2023) 318–326.
[10] S.M. Hazaveie, G. Sodeifian, N. Saadati Ardestani, Micro and nanosizing of tamsulosin drug via supercritical CO2 antisolvent (SAS) process, J. CO2 Utilization 84 (2024) 102847.
[11] M. Mirzaie, et al., Experimental measurement and thermodynamic/intelligent modeling of yellow 2 G solubility in supercritical carbon dioxide with/without co-solvent, Chem. Eng. Res. Des. 207 (2024) 160–180.
[12] M. Amani, N. Saadati Ardestani, S.A. Sajadian, Production of dye nanoparticles via a supercritical gas anti-solvent process and optimisation of the process conditions, Color. Technol. 139 (6) (2023) 703–718.
[13] N. Saadati Ardestani, et al., Solubility of famotidine in supercritical carbon dioxide: experimental measurement and thermodynamic modeling, J. Supercrit. Fluids 201 (2023) 106031.
[14] G. Sodeifian, et al., Determination of gefitinib hydrochloride anti-cancer drug solubility in supercritical CO2: evaluation of sPC-SAFT EoS and semi-empirical models, J. Taiwan Inst. Chem. Eng. 161 (2024) 105569.
[15] S. Ali Sajadian, et al., Experimental analysis and thermodynamic modelling of lenalidomide solubility in supercritical carbon dioxide, Arab. J. Chem.15 (2022) 103821.
[16] R.S. Alwi, et al., Experimental study and thermodynamic modeling of clonazepam solubility in supercritical carbon dioxide, Fluid Phase Equilib. 574 (2023) 113880.
[17] M. Amani, et al., Solubility measurement of the fludrocortisone acetate in supercritical carbon dioxide: experimental and modeling assessments, J. Supercrit. Fluids 190 (2022) 105752.
[18] M.A.S. Abourehab, et al., Laboratory determination and thermodynamic analysis of alendronate solubility in supercritical carbon dioxide, J. Mol. Liq. 367 (2022) 120242.
[19] M. Amani, N. Saadati Ardestani, Investigation of the solubility of anticancer drugs in the supercritical solvent for development of innovative drug delivery systems; artificial intelligence paradigms (MLP-ANN) and thermodynamic correlations, J. Mol. Liq. 394 (2024) 123701.

[20] N.S. Ardestani, et al., Theoretical and experimental study on chloroquine drug solubility in supercritical carbon dioxide via the thermodynamic, multi-layer perceptron neural network (MLPNN), and molecular modeling, Arab. J. Chem. 15 (12) (2022) 104371.
[21] G. Sodeifian, et al., Determination of regorafenib monohydrate (colorectal anticancer drug) solubility in supercritical CO2: experimental and thermodynamic modeling, Heliyon 10 (8) (2024) e29049.
[22] A. Rojas, et al., Solubility of oxazepam in supercritical carbon dioxide: experimental and modeling, Fluid Phase Equilib. 585 (2024) 114165.
[23] K. Venkatesan, et al., Experimental - theoretical approach for determination of metformin solubility in supercritical carbon dioxide: thermodynamic modeling, Case Stud. Therm. Eng. 41 (2023) 102649.
[24] Y. Yamini, J. Hassan, S. Haghgo, Solubilities of some nitrogen-containing drugs in supercritical carbon dioxide, J. Chem. Eng. Data 46 (2) (2001) 451–455.
[25] S.A. Sajadian, et al., Solubility measurement and correlation of alprazolam in carbon dioxide with/without ethanol at temperatures from 308 to 338 K and pressures from 120 to 300 bar, J. Chem. Eng. Data 69 (4) (2024) 1718–1730.
[26] G. Soave, Equilibrium constants from a modified Redlich-Kwong equation of state, Chem. Eng. Sci. 27 (6) (1972) 1197–1203.
[27] J.-S. Cheng, M. Tang, Y.-P. Chen, Correlation of solid solubility for biological compounds in supercritical carbon dioxide: comparative study using solution model and other approaches, Fluid Phase Equilib. 194-197 (2002) 483–491.
[28] L.L. Williams, J.B. Rubin, H.W. Edwards, Calculation of Hansen solubility parameter values for a range of pressure and temperature conditions, including the supercritical fluid region, Ind. Eng. Chem. Res. 43 (16) (2004) 4967–4972.
[29] G. Sodeifian, et al., Solubility of pazopanib hydrochloride (PZH, anticancer drug) in supercritical CO2: experimental and thermodynamic modeling, J. Supercrit. Fluids 190 (2022) 105759.
[30] J. Marrero, R. Gani, Group-contribution based estimation of pure component properties, Fluid Phase Equilib. 183-184 (2001) 183–208.
[31] G. Sodeifian, et al., Experimental data and thermodynamic modeling of solubility of azathioprine, as an immunosuppressive and anti-cancer drug, in supercritical carbon dioxide, J. Mol. Liq. 299 (2020) 112179.
[32] G. Sodeifian, F. Razmimanesh, S.A. Sajadian, Solubility measurement of a chemotherapeutic agent (imatinib mesylate) in supercritical carbon dioxide: assessment of new empirical model, J. Supercrit. Fluids 146 (2019) 89–99.
[33] G. Sodeifian, et al., Experimental and thermodynamic analyses of supercritical CO2-solubility of minoxidil as an antihypertensive drug, Fluid Phase Equilib. 522 (2020) 112745.
[34] Y. Yu, C. Sun, W. Jiang, A comprehensive study of pharmaceutics solubility in supercritical solvent through diverse thermodynamic and hybrid machine learning approaches, Int. J. Pharm. 664 (2024) 124579.
[35] G. Sodeifian, et al., Determination of the solubility of the repaglinide drug in supercritical carbon dioxide: experimental data and thermodynamic Modeling, J. Chem. Eng. Data 64 (12) (2019) 5338–5348.
[36] F. Arabgol, et al., Experimental and thermodynamic investigation of gemifloxacin solubility in supercritical CO2 for the production of nanoparticles, J. Supercrit. Fluids 206 (2024) 106165.
[37] A.J. Obaidullah, A.A. Almehizia, Analysis experimental and modeling of the solubility of an antiepileptic drug, levetiracetam, in supercritical solvent, J. Mol. Liq. 390 (2023) 123065.
[38] S.A. Sajadian, N.S. Ardestani, A. Jouyban, Solubility of montelukast (as a potential treatment of COVID -19) in supercritical carbon dioxide: experimental data and modelling, J. Mol. Liq. 349 (2022) 118219.
[39] Z. Alhuwaymil, et al., Measurement and Modeling of zolpidem solubility in supercritical carbon dioxide: effect of two cosolvents, J. Chem. Eng. Data 69 (5) (2024) 1966–1983.
[40] A. Immirzi, B. Perini, Prediction of density in organic crystals, Acta Crystallogr. A 33 (1) (1977) 216–218.
[41] C.-Y. Hsu, et al., Comprehensive study of medications solubility in supercritical CO2 with and without CO-solvent; laboratory, theoretical, and intelligent approaches, J. Mol. Liq. 411 (2024) 125765.
[42] W.C. Edmister, Applied Hydrocarbon Thermodynamics, Part 4: Compressibility Factors and Equations of State, Gulf Publishing Company, 1961.
[43] G. Sodeifian, et al., Prediction of solubility of sodium valproate in supercritical carbon dioxide: experimental study and thermodynamic Modeling, J. Chem. Eng. Data 65 (4) (2020) 1747–1760.
[44] D. Mackay, et al., Vapor-pressure correlations for low-volatility environmental chemicals, Environ. Sci. Technol. 16 (10) (1982) 645–649.
[45] S. Verheyen, et al., Determination of partial solubility parameters of five benzodiazepines in individual solvents, Int. J. Pharm. 228 (1) (2001) 199–207.
[46] C.M. Wassvik, et al., Molecular characteristics for solid-state limited solubility, J. Med. Chem. 51 (10) (2008) 3035–3039.
[47] M.A. Khan, et al., Study of baclofen solubility in supercritical CO_2 with and without cosolvents: experimental analysis, thermodynamic evaluation, and machine learning methods, J. Chem. Eng. Data,70 (2) (2025) 953–971.
[48] Y. Zhang, X. Xu, Machine learning bioactive compound solubilities in supercritical carbon dioxide, Chem. Phys. 550 (2021) 111299.
[49] M. Soleimani Lashkenari, A. KhazaiePoul, Application of KNN and semi-empirical models for prediction of polycyclic aromatic hydrocarbons solubility in supercritical carbon dioxide, Polycycl. Aromat. Compd. 37 (5) (2017) 415–425.
[50] S.M. Alshahrani, et al., Application of CO2 supercritical fluid to optimize the solubility of Oxaprozin: development of novel machine learning predictive models, Molecules (2022) 27, https://doi.org/10.3390/molecules27185762.
[51] A. Zhu, et al., Political optimizer with interpolation strategy for global optimization, PLoS One 16 (2021) e0251204.
[52] J. Dong, et al., A hybrid greedy political optimizer with fireworks algorithm for numerical and engineering optimization problems, Sci. Rep. 12 (1) (2022) 13243.
[53] J.D. Van der Waals, Over de Continuiteit Van Den Gas-en Vloeistoftoestand (On the Continuity of the Gas and Liquid State), University of Leiden, 1873.
[54] M. Askarizadeh, et al., Binary and ternary approach of solubility of rivaroxaban for preparation of developed nano drug using supercritical fluid, Arab. J. Chem. 17(4) (2024) 105707.
[55] M. Bazaei, et al., Measurement and thermodynamic modeling of solubility of erlotinib hydrochloride, as an anti-cancer drug, in supercritical carbon dioxide, Fluid Phase Equilib. 573 (2023) 113877.
[56] N. Esfandiari, S. Ali Sajadian, Solubility of Lacosamide in supercritical carbon dioxide: an experimental analysis and thermodynamic modeling, J. Mol. Liq. 360 (2022) 119467.
[57] N.S. Ardestani, et al., Experimental and modeling of solubility of sitagliptin phosphate, in supercritical carbon dioxide: proposing a new association model, Sci. Rep. 13 (1) (2023) 17506.
[58] N.S. Ardestani, N.Y. Majd, M. Amani, Experimental measurement and thermodynamic Modeling of capecitabine (an anticancer drug) solubility in supercritical carbon dioxide in a ternary system: effect of different cosolvents, J. Chem. Eng. Data 65 (10) (2020) 4762–4779.
[59] N. Saadati Ardestani, M. Amani, L. Moharrery, Determination of anthraquinone violet 3RN solubility in supercritical carbon dioxide with/without co-solvent: experimental data and modeling (empirical and thermodynamic models), Chem. Eng. Res. Des. 159 (2020) 529–542.
[60] G. Sodeifian, et al., Experimental investigation and modeling of the solubility of oxcarbazepine (an anticonvulsant agent) in supercritical carbon dioxide, Fluid Phase Equilib. 493 (2019) 160–173.
[61] G. Sodeifian, et al., Solubility of palbociclib in supercritical carbon dioxide from experimental measurement and Peng–Robinson equation of state, Sci. Rep. 13 (1) (2023) 2172.
[62] B. Luo, et al., Experimental validation and modeling study on the drug solubility in supercritical solvent: case study on exemestane drug, J. Mol. Liq. 377 (2023) 121517.
[63] S.A. Shojaee, et al., Experimental investigation and modeling of the solubility of carvedilol in supercritical carbon dioxide, J. Supercrit. Fluids 81 (2013) 42–47.
[64] Y. Alghazwani, et al., Investigating the thermal enhancement of levetiracetam solubility in the ternary system of supercritical carbon dioxide and ethanol, J. Mol. Liq. 411 (2024) 125692.
[65] Z. Huang, et al., Solubility of aspirin in supercritical carbon dioxide with and without acetone, J. Chem. Eng. Data 49 (5) (2004) 1323–1327.